

A novel 3D BE formulation for general multi-zone domains under body force loading

Mohammad Ghiasian* and Mohammad Taghi Ahmadi^a

Department of Civil and Environmental Engineering, Tarbiat Modares University, Tehran 14115-397, Iran

(Received May 8, 2013, Revised November 4, 2013, Accepted November 9, 2013)

Abstract. The current paper proposes a boundary element formulation, applicable to 2-D and 3-D elastostatics problems using a unified approach for transformations of the domain integrals into boundary integrals. The method is applicable to linear problems encompassing both finite and infinite multi-region domains allowing non-vanishing body forces. Numerical results agree quite well with the analytical solutions; while the present method offers easy formulation with less numerical efforts in comparison to FEM or some BEM which need interior points to treat arbitrary body forces. It is demonstrated that the method has the potential to have profound impact on engineering design, notably in dam-foundation interaction.

Keywords: boundary element method; elastostatics; multi-zone structures; body force

1. Introduction

In many practical problems of soil-structure interaction, the soil is modeled as a homogeneous, isotropic and linearly elastic half-space. Thus the class of problems amenable to analytical solutions is quite limited and therefore numerical methods of solution are imperative for problems associated with complex geometry, boundary conditions and loading. The most popular numerical method is the finite element method (FEM). However, for the solution of problems involving a semi-infinite or infinite medium, FEM or FDM (finite-difference method) exhibit a deficiency because one has to employ a mesh of finite size which needs approximate far boundary conditions. An alternative approach for the numerical analysis of the aforementioned problems is the boundary element method (BEM). Although BEM needs no discretization inside the domain, but it suffers from certain shortcomings: loads may only be applied at boundaries, and not inside the domain. Thus a number of complications should be overcome when body forces such as gravity, seepage or centrifugal forces have to be considered. Although some researchers have studied elasticity with arbitrary body forces by BEM, but they mainly dealt with two dimensional applications or purely axisymmetric elastostatics problems. They usually used the dual reciprocity BEM formulations, or particular integrals to eliminate the domain integrals (Deb and Banerjee 1990, Park and Banerjee 2002, Ochiai and Kobayashi 2000, Perez-Gavilon and Aliabadi 2001, Park 2002).

*Corresponding author, Ph.D. Student, E-mail: m.ghiasian@modares.ac.ir

^aProfessor, E-mail: mahmadi@modares.ac.ir

Recently, several researchers have studied boundary element methods in elastostatics problems to propose new methods reducing the errors resulted from the numerical calculation of integrals (Milroy *et al.* 1997, Tang and Fenner 2005, Simpson *et al.* 2013), the time and memory needed for the analysis (Maerten 2010) or to resolve singularities inherent to BEM using either indirect (Shen 2011, Cheng and Shuwei 2012) or semi-analytical methods (Khodakarami 2011). However, for simplicity, they neglected the body forces to remove the volume integral.

This paper proposes a method to include, with ease; the general body forces in the direct three-dimensional BE model including finite or infinite multi-region domains. The method could deal with essential geotechnical loads such as gravity, initial stress, seepage, buoyancy and even centrifugal forces, or any arbitrary body forces due to potential functions with linear spatial variation. The method employs a fairly straight forward transformation of volume integrals into surface integrals. Despite previous works, the method suits particularly for multi-region problems with infinite domains. Some practical applications to dam-foundation interaction are presented to prove its versatility and precision.

2. Governing equations

Boundary value problems with body force for 3D multi region elastostatics are considered. The material for each region is homogeneous, isotropic, linear elastic and the domain may be finite or infinite.

The equations of equilibrium are stated as

$$\sigma_{ij,j} + b_i = 0, \quad i, j = 1, 2, 3, \quad (1)$$

where σ_{ij} are the Cauchy stress tensor and b_i denotes the components of the body-force. Assuming small displacements, strains ϵ_{ij} are defined by

$$\epsilon_{ij} = \frac{1}{2}(u_{i,j} + u_{j,i}), \quad i, j = 1, 2, 3, \quad (2)$$

u_i represents a displacement component, and commas imply differentiation. In addition to Eq. (2), strains have to satisfy the following compatibility equations (Timoshenko and Goodier 1970)

$$\frac{\partial \epsilon_{ij}}{\partial X_j \partial X_k} - \frac{\partial}{\partial X_i} \left(-\frac{\partial \epsilon_{jk}}{\partial X_i} + \frac{\partial \epsilon_{ik}}{\partial X_j} + \frac{\partial \epsilon_{ij}}{\partial X_k} \right) = 0 \quad (3)$$

where i, j , and k count from 1 to 3, but $i \neq j \neq k$.

One of the most common ways of deriving the BE formulation is to utilize Betti's reciprocal theorem which states that, given two loading states $\sigma_{ij}, \epsilon_{ij}$ and $\sigma_{ij}^*, \epsilon_{ij}^*$ then these can be related (assuming linear elasticity) as

$$\int_V \sigma_{ij} \epsilon_{ij}^* d\Omega = \int_V \sigma_{ij}^* \epsilon_{ij} d\Omega \quad (4)$$

V denotes the domain with the boundary S of the problem. Applying the divergence theorem and using equilibrium Eq. (1), the displacement-strain relation (2), and the definition of tractions given by $t_i = \sigma_{ij} n_j$, the integral representation for the displacement \mathbf{u} at a point P on the boundary of an elastic body, with body force \mathbf{b} and zero initial conditions can be written as (Aliabadi 2002)

$$\mathbf{c}\mathbf{u}(P) = \int_S \mathbf{U}(P, Q)\mathbf{t}(Q)dS - \int_S \mathbf{T}(P, Q)\mathbf{u}(Q)dS + \int_V \mathbf{U}(P, \bar{Q})\mathbf{b}(\bar{Q})dV \quad (5)$$

where \mathbf{u} and \mathbf{t} stand for the displacement and traction vectors, respectively; $\mathbf{U}(P, Q)$ and $\mathbf{T}(P, Q)$ are the fundamental solution displacement and traction tensors, respectively, at point Q due to a point load at P . The coefficient \mathbf{c} only depends on the geometry at point Q on the boundary, and \bar{Q} is a point within the domain. The fundamental solution tensors are

$$U_{i,j}(P, Q) = C(C_1\delta_{ij} + r_i r_j) \quad (6)$$

with

$$C = \frac{1}{16\pi\mu(1-\nu)}, \quad C_1 = 3 - 4\nu \quad (7)$$

and

$$T_{ij}(P, Q) = \frac{C_2}{r^2} [C_3\delta_{ij} + 3r_i r_j \cos\theta - C_3(1 - \delta_{ij})(n_j r_i - n_i r_j)] \quad (8)$$

with

$$C_2 = \frac{1}{8\pi(1-\nu)}, \quad C_3 = 1 - 2\nu \quad (9)$$

The last integral in Eq. (5) is a volume integral. It can be shown that for constant body forces over volume V , this integral can be transformed into a surface integral (Brebbia *et al.* 1984)

$$\int_V \mathbf{U}(P, Q)\mathbf{b}(Q)dV = \int_S \mathbf{G}ds \quad (10)$$

For 3-D problems the coefficients of \mathbf{G} may be computed from (Beer *et al.* 2008)

$$G_i = \frac{1}{8\pi\mu} \left(b_i \cos\theta - \frac{1}{2(1-\nu)} n_i \cos\psi \right) \quad (11)$$

where $x, y,$ and z may be substituted for i, μ is the shear modulus and

$$\cos\psi = \mathbf{b} \cdot \frac{1}{r} \mathbf{r} \quad (12)$$

\mathbf{r} is the position vector and n_i denotes the components of the outward normal to the boundary S .

For plane strain problems (Beer *et al.* 2008) we have

$$G_i = \frac{1}{8\pi\mu} \left(2\ln\frac{1}{r} - 1 \right) \left(b_i \cos\theta - \frac{1}{2(1-\nu)} n_i \cos\psi \right) \quad (13)$$

To allow for numerical implementation, we discretize the boundary into a non-overlapping set of N_e elements giving

$$S = \bigcup_{e=1}^{N_e} S_e, \quad S_i \cap S_j = 0, \quad i \neq j \quad (14)$$

To arrive at a system of equations, the conventional procedure is to use collocation at a series of points around the boundary. This corresponds to placing the point P at a discrete set of points;

most often, for classical (i.e., unenriched) BE formulations the nodal positions, since this automatically provides a square set of equations. In this way, the system of equations can be written in matrix notation as

$$[\mathbf{T}]\{\mathbf{u}\} = [\mathbf{U}]\{\mathbf{t}\} \quad (15)$$

where $[\mathbf{T}]$ is a square matrix containing a combination of the integrals of the T_{ij} kernel and the jump terms, $\{\mathbf{u}\}$ is vector of displacement components, $[\mathbf{U}]$ is a rectangular matrix of U_{ij} kernel integrals, and $\{\mathbf{t}\}$ is a vector of traction components. Rearranging this set of equations by placing all unknown components on the left-hand side and all known components on the right hand side, the following is found

$$[\mathbf{A}]\{\mathbf{X}\} = \{\mathbf{F}\} \quad (16)$$

where the vector \mathbf{x} contains all unknown displacement and traction components.

The analysis of problems with constant body forces proceeds the same way, except that an additional right hand side term is assembled. The final system of equations will be

$$[\mathbf{A}]\{\mathbf{X}\} = \{\mathbf{F}\} + \{\mathbf{F}\}_b \quad (17)$$

where the components of \mathbf{F}_b for the i -th collocation point are

$$F_{ib} = \sum_{e=1}^E \Delta G_i^e \quad (18)$$

and

$$\Delta G_i^e = \int_{S_e} \mathbf{G}(P_i, Q) dS(Q) \quad (19)$$

The discretized form of Eq. (5) can be written as

$$\mathbf{c}\mathbf{u}(P_i) + \sum_{e=1}^E \sum_{n=1}^N \Delta T_{ni}^e \mathbf{u}_n^e = \sum_{e=1}^E \sum_{n=1}^N \Delta U_{ni}^e \mathbf{t}_n^e + \sum_{e=1}^E \Delta G_i^e \quad (20)$$

Eq. (17) may then be solved using an appropriate solver.

3. Boundary elements in multi region problems

In usual fundamental solutions it is assumed that material properties do not change inside the domain being analyzed and thus they are only applicable to homogeneous domains. There are many instances, however, where this assumption does not hold. For example, in a soil or rock mass body, the modulus of elasticity may change with depth or from one layer to the other. For some special types of heterogeneity it is possible to derive fundamental solutions, if the material properties change in a simple way (e.g., when linearly increasing with depth). However, such fundamental solutions are often complicated and the programming efforts significant. In cases where we have layers or zones of different materials, however, we can develop special solution methods based on the fundamental solutions for homogeneous materials. The basic idea is to consider a number of regions connected to each other, much like pieces of a puzzle. Each region is treated in the same way but can now be assigned with a different material property and thus we are

able to solve piecewise homogeneous material problems (Beer and Poulsen 1994). Since at the interfaces between the regions both traction and displacement are not known, the total number of unknowns is increased and additional equations are required to solve the problem. The latter equations could be obtained from the conditions of equilibrium and compatibility at the region interfaces (Aliabadi 2002).

In addition to Eq. (5), another integral equation, written in terms of tractions, may be used dealing with contact problems (Leonel and Venturini 2010a). This equation can be obtained from Eq. (5), which must be differentiated to obtain the integral representation in terms of strains. Then, Hooke's law is applied to obtain the integral representation in terms of stresses. Finally, multiplication by the director cosines of the normal to contact surfaces at the collocation point leads to the traction representation, as follows

$$\frac{1}{2}\mathbf{t}(P) = \mathbf{n} \int_S \mathbf{D}(P, Q)\mathbf{t}(Q)dS - \mathbf{n} \int_S \mathbf{S}(P, Q)\mathbf{u}(Q)dS + \mathbf{n} \int_V \mathbf{D}(P, \bar{Q})\mathbf{b}(\bar{Q})dV \quad (21)$$

where \mathbf{n} is the unit outward normal vector, the fundamental solutions of \mathbf{D} and \mathbf{S} are obtained from the matrices \mathbf{U} and \mathbf{T} by applying the definition of tractions (Aliabadi 2002), and the second integral on the right hand side contains hyper singular integrands.

Generally three schemes are used for dealing with multi-zone contacts. In the first scheme, called SST (Leonel and Venturini 2011), only algebraic relations derived from the integral expression written in terms of displacements, i.e., Eq. (5), are used.

The second scheme is the HST scheme in which for external boundaries only algebraic equations derived from the singular integral equation, i.e., Eq. (5) are used, while along contact surfaces only algebraic equations derived from the hyper singular integral equation, Eq. (21), are used. An alternative scheme, namely THST, has been also proposed in which all the algebraic relations along the contact surfaces and along external boundaries are founded on the hyper singular integral equation, Eq. (21).

It is worth to emphasize that when algebraic relations are obtained from Eq. (21), discontinuous elements must be used to approximate tractions and displacements. As the hyper-singular integral equation can be approximated only if the derivatives of the displacement function are continuous in the vicinity of the source point, the nodes should be defined inside the elements. However in the case of SST approach, continuous elements can be adopted for all boundaries.

Moreover, as shown in Leonel and Venturini (2011), the model uses only algebraic equations coming from singular integral representation. It has demonstrated to be more accurate when compared with other works, especially in nonlinear contacts. Such superiority of SST might be due to higher singularity level present in the algebraic equations of the HST and THST schemes, in respect to that of the SST approach. Therefore, in the present research the SST approach is employed, which is appropriate for both linear and non-linear contact problems, while the HST and THST methods are more popular in the fracture mechanics (Beer 1993, Leonel and Venturini 2010b).

There are two approaches how to implement the SST method. In the first, we modify the assembly procedure, so that a larger system of equations is now obtained including the additional unknowns at the interfaces. The second approach is similar to the approach taken in the finite element method (Banerjee 1994, Kuo and Chen 2005, Rodriguez-Tembleque and Abascal 2010).

Here we construct a "stiffness matrix", \mathbf{K} , for each region, the coefficients of which are the tractions due to unit displacements (Pereira and Beer 2009). The matrices \mathbf{K} for all regions are then assembled in the same way as in FEM. The second method may be naturally used for

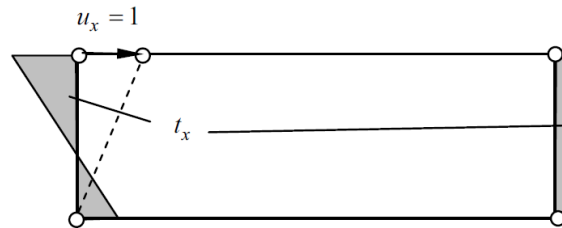


Fig. 1 Example of computation of “stiffness coefficients”

coupling some boundaries with finite elements. The method is also more efficient and more amenable for parallel computing, and consequently the stiffness matrix approach is proposed in this paper.

3.1 Stiffness matrix assembly

The idea is to compute a “stiffness matrix” \mathbf{K}^N for each region N . Coefficients of \mathbf{K}^N are values of \mathbf{t} due to unit values of \mathbf{u} at all region nodes. In elasticity problems these would correspond to tractions due to unit displacements. To obtain the “stiffness matrix” \mathbf{K}^N of a region, we simply solve the Dirichlet problem M times, where M is the number of degrees of freedom of the BE region nodes. For example, to get the first column of \mathbf{K}^N , we apply a unit value of displacement in x -direction, as shown in Fig. 1, while setting all other node values to zero.

For computation of Dirichlet problems we recall Eq. (15), with a modified right hand side

$$[\Delta\mathbf{U}]\{\mathbf{t}\}_1 = [\Delta\mathbf{T}]\{\mathbf{u}\}_1 \quad (22)$$

here $[\Delta\mathbf{T}]$, and $[\Delta\mathbf{U}]$ are the assembled coefficient matrices, $\{\mathbf{t}\}_1$ is the first column of the stiffness matrix \mathbf{K}^M , and $\{\mathbf{u}\}_1$ a vector with a unit value in the first row, i.e.

$$\{\mathbf{u}\}_1 = \begin{Bmatrix} 1 \\ 0 \\ 0 \\ \vdots \\ \vdots \end{Bmatrix} \quad (23)$$

If we perform the multiplication of $[\Delta\mathbf{T}]\{\mathbf{u}\}_1$, it can be easily seen that the right hand side of Eq. (22) is simply the first column of matrix $[\Delta\mathbf{T}]$. The computation of the region “stiffness matrix” is therefore basically a solution of $[\Delta\mathbf{U}]\{\mathbf{t}\}_i = \{\mathbf{F}\}_i$ with N right hand side vectors $\{\mathbf{F}\}_i$, where each right hand side corresponds to a column in $[\Delta\mathbf{T}]$. Each solution vector $\{\mathbf{t}\}_i$ represents a column in \mathbf{K} , i.e.

$$\mathbf{K}^N = [\{\mathbf{t}\}_1 \{\mathbf{t}\}_2 \dots] \quad (24)$$

For each region N , we have the following relationship between $\{\mathbf{t}\}$ and $\{\mathbf{u}\}$

$$\{\mathbf{t}\}^N = \mathbf{K}^N \{\mathbf{u}\}^N \quad (25)$$

3.2 Partially coupled problems

In many cases we have problems where not all nodes of the regions are connected. Here only some of the nodes of one region are connected to other regions. It is obviously more efficient in the calculation of the stiffness matrix to consider only the interface nodes, i.e., only nodes connected to other regions. For partially coupled problems we therefore have to solve the following two problems;

First, the prescribed boundary conditions are applied only to nodes not connected to other regions (free nodes), and at the same time zero-value Dirichlet boundary conditions are applied to nodes connected to other regions (coupled nodes).

The second problem to be solved (for each region), is to apply Dirichlet boundary conditions of unit value to coupled nodes and zero-value to free nodes.

After all regional stiffness matrices \mathbf{K}^N have been computed, they are assembled to form a system of equations established on the conditions of equilibrium and compatibility. This results in the following system of equations

$$[\mathbf{K}]\{\mathbf{u}\}_c = \{\mathbf{F}\} \tag{26}$$

where $[\mathbf{K}]$ is the assembled “stiffness matrix” of the interface nodes and $\{\mathbf{F}\}$ is the assembled right hand side vector. This problem is solved for the unknown $\{\mathbf{u}\}_c$ at all interfaces nodes of the system.

After the interfaces unknowns have been determined, the values of \mathbf{t} at the interface, denoted by $\{\mathbf{t}\}_c^N$ and the values of \mathbf{u} , or \mathbf{t} at the free nodes, denoted by $\{\mathbf{x}\}_f^N$, are determined for each region. These are obtained by the application of

$$\begin{Bmatrix} \{\mathbf{t}\}_c^N \\ \{\mathbf{x}\}_f^N \end{Bmatrix} = \begin{Bmatrix} \{\mathbf{t}\}_{c0}^N \\ \{\mathbf{x}\}_{f0}^N \end{Bmatrix} + \begin{bmatrix} \mathbf{K}^N \\ \mathbf{A}^N \end{bmatrix} \{\mathbf{u}\}_c^N \tag{27}$$

where matrices \mathbf{K}^N and \mathbf{A}^N are defined by

$$\mathbf{K}^N = [\{\mathbf{t}\}_{c1} \quad \dots \quad \{\mathbf{t}\}_{cN_c}]^N \tag{28}$$

and

$$\mathbf{A}^N = [\{\mathbf{x}\}_{c1} \quad \dots \quad \{\mathbf{x}\}_{cN_c}]^N \tag{29}$$

Vector $\{\mathbf{t}\}_{c0}^N$ contains the tractions at the coupled nodes, and vector $\{\mathbf{x}\}_{f0}^N$ contains either both displacements and tractions at the free nodes of region N , depending on the boundary conditions prescribed with fixed interface nodes.

Note that $\{\mathbf{u}\}_c^N$ is obtained by gathering values from the vector of unknowns at all the interfaces $\{\mathbf{u}\}_c$.

4. Results

4.1 Validation of the method

4.1.1 Circular excavation in infinite domain

Consider a cavity inside an infinite, homogeneous, and elastic space. The elastic space is

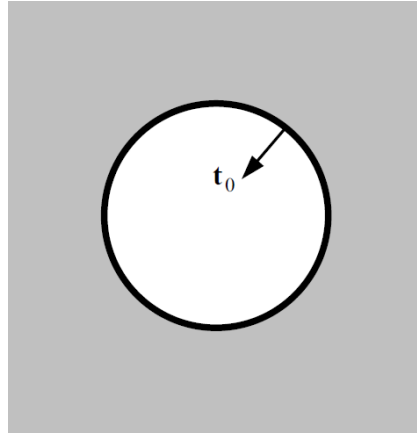


Fig. 2 Circular cavity inside infinite domain

Table 1 Response around circular cavity inside infinite domain

	Max. Displacement (mm)	Max. Stress (MPa)
BEM	0.600	-9.000
FEM	0.506	-8.165
Theory	0.600	-9.000

assumed to have a modulus of elasticity of 10 GPa, a Poisson's ratio of zero, and an initial stress field of $\sigma_x = 0.0$ MPa, $\sigma_y = -3.0$ MPa, $\tau_{xy} = 0.0$ MPa as shown in Fig. 2.

Twelve parabolic boundary elements are used to model the circular cavity. Maxima of stress and displacement due to excavation are obtained and compared with those of the FEM, and the theoretical solution. In the FE model, 64 quadratic elements of the same size as that of the BEs are employed. A truncation boundary at distance of two diameters away from the excavation is used. At the truncation surface all displacements are assumed as fixed.

It is seen that FE model introduces two sources of error; one associated with the truncation of the medium due to disability of modeling the infinite domain, and the other associated with the shape functions approximations inside the continuum as well as along the boundary surfaces (Beer *et al.* 2008). The results are shown in Table 1.

4.1.2 Multi-region domain solution

In next example, a cantilever beam consisting of two regions is specified under applied shear traction at its end as shown in Fig. 3.

For comparison with theoretical results, both the regions have the same properties as $E = 10$ GPa, and $\nu = 0.0$. The beam end shear traction is 10 kN/m.

It can be seen that the maximum displacement is 0.5012m, as compared with the theoretical value of 0.500m, and that the multi-region method does not result in any loss of accuracy.

4.1.3 Self-weight in a soil

In order to test the body force formulation, an example of application for gravitational forces is given and the results are compared with their analytical and numerical solutions. The example deals the problem of finding stresses in the elastic soil body due to its own weight (Fig. 4).

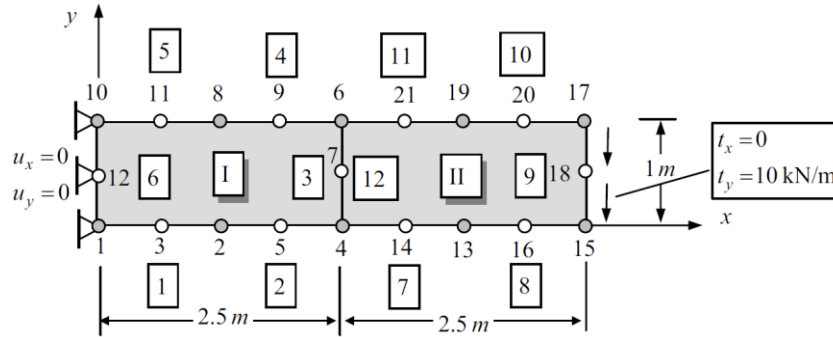


Fig. 3 Cantilever beam multi-region mesh

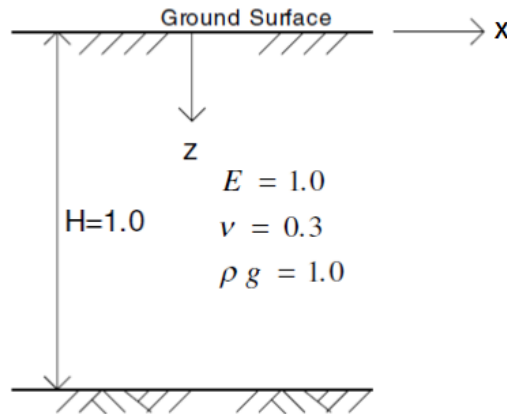


Fig. 4 Self-weight in a soil

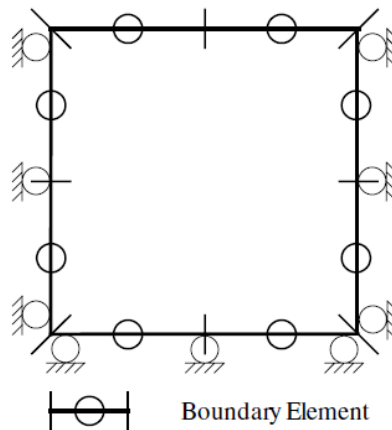


Fig. 5 Typical modeling mesh for self-weight problem in a soil

The bottom and lateral sides of the soil are restrained for normal displacement by using roller boundary condition and modeled with eight parabolic boundary elements shown in Fig. 5.

Table 2 Numerical results for self-weight problem in a soil

	Analytical Solution	2D BEM Model (Park 2002) (Error Percentage)	Present BEM Model (Error Percentage)
u_z at $z=0$	0.371	0.382 (3.0%)	0.379 (2.2%)
σ_z at $z = H$	1.000	1.028 (2.8%)	1.017 (1.7%)
σ_x at $z = H$	0.429	0.441 (2.8%)	0.437 (1.9%)

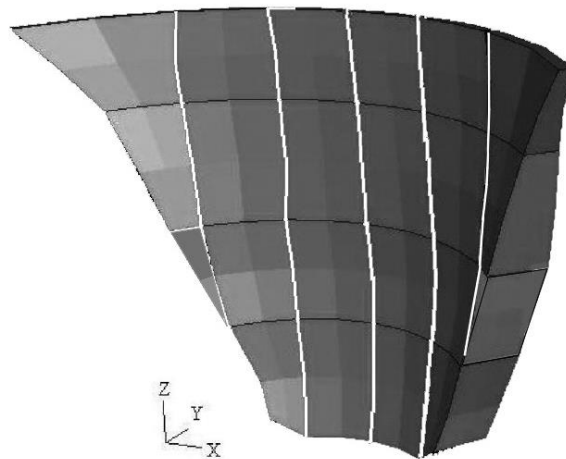


Fig. 6 Model of Morrow Point arch dam

Numerical results for settlement at the top surface and stresses at the bottom are compared with analytical solutions and the 2D axisymmetric BEM model including 3 interior points in Table 2 (Park 2002). Better agreement can be seen in present formulation analysis in comparison with results from the 2D BEM model using particular integrals, while it includes some interior points.

4.2 Numerical examples for general application of the method

4.2.1 Static loading of an arch dam

The well-studied Morrow Point arch dam of 141.73 m height is considered under static loading. The loads consist of the dam body weight load and the reservoir hydrostatic pressure. Modulus of elasticity and poisson ratio of concrete are 26 GPa and 0.2, respectively. Concrete and water unit mass values are also 2400 and 1000 kg/m³. Assuming rigid foundation, BEM results are compared against those of the FEM published by Ahmadi *et al.* (2001) as shown in Table 3. Boundary element model employed here is composed of 6 coupled regions (defined by vertical contraction joints) containing 62 linear 3D surface elements, while the FE model is constructed of a single layer of 22 quadratic elements. These results depict a notable agreement between the two methods, i.e., the multi-region BEM and the standard FEM.

4.2.2 Multi-region unbounded foundation interaction of an arch dam

Further analysis including the unbounded foundation and the same dam is conducted next under the same type of loads and dam elements. Here dissimilar to dam engineering practice in linear analysis, foundation weight load is included. Deformability of the foundation rock is

Table 3 Results of Morrow Point dam analyses with rigid foundation

	Max. U/S Tensile Arch Stress (MPa)	Max. D/S Compression Cantilever Stress (MPa)	Max. Displacement of the Dam Crest (mm)
BEM	0.4	6.5	25
FEM	0.3	6.7	27

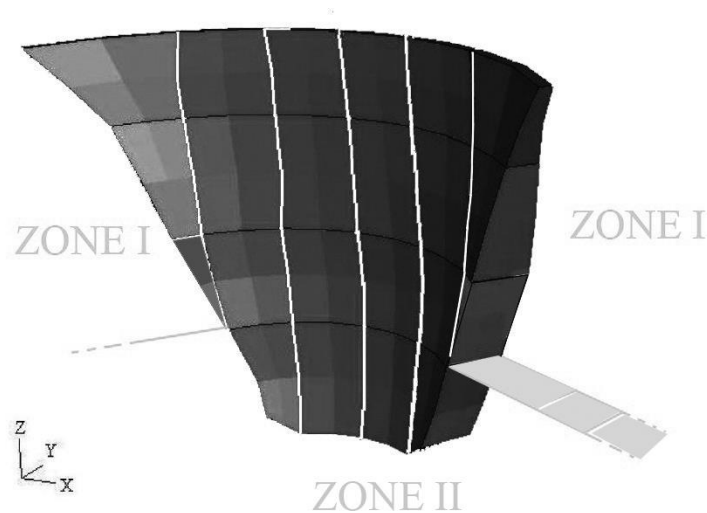


Fig. 7 Model of Morrow Point arch dam and its foundation

characterized by the modulus of deformation or elasticity. Depending on the type of material and discontinuities present in a foundation, values of the modulus of elasticity may vary significantly from abutment to abutment, or with elevations. The presented BE algorithm is used to survey the effects of the dam-foundation interaction effects on the response of the dam. Nine cases are being analysed as cases I to IX. In all cases the foundation free-field boundary elements are extended in each side of the dam by a length of three times the dam height. In the first five cases E_I and E_{II} , moduli of elasticity of abutments, and the lower foundation are the same and equal to constant value of E_f . However, in the next three analyses the abutment (zone I) is assumed to be weaker than the lower foundation (zone II) as in Fig. 7. Case IX is analyzed to compare the effects of foundation and abutment stiffness on the response of the arch dam. In this case, the lower foundation is assumed to be weak and the left and the right abutments strong. The dam properties are same as in section 4.2.1, and abutment and foundation properties are shown in Table 4.

The results in Table 4 demonstrate that the dam deflections and stresses are more sensitive to foundation modulus ratios E_f/E_c of less than 1.0. Such responses especially increase dramatically when E_f/E_c becomes less than 0.5; while dam deflections for stiffer foundation rock is practically tending to those for a rigid foundation. For such uniform isotropic foundations, under gravity and hydrostatic loading, foundation flexibility increases arch stresses mostly in the central part of the upstream and on the lower part of the downstream faces of the dam, while cantilever stresses are primarily increased in the lower 1/3 portion of the dam.

At some dam sites, the foundation modulus may vary significantly with elevation. In the next three cases variable foundation modulus with regard to zones I and II is being studied. Sensitivity

Table 4 Morrow Point Dam-foundation system analyses cases and response sensitivities to foundation parameters

Analyses Cases	Case I	Case II	Case III	Case IV	Case V	Case VI	Case VII	Case VIII	Case IX
E_{II}/E_c	0.25	0.5	1.0	2.0	Rigid	1.0	2.0	4.0	0.25
E_I/E_c	0.25	0.5	1.0	2.0	Rigid	0.5	1.0	0.25	4.0
Max. U/S Tensile Arch Stress (MPa)	0.9	0.6	0.5	0.4	0.4	0.6	0.5	1.4	1.0
Max. D/S Compression Cantilever Stress (MPa)	12.3	8.7	7.3	6.3	6.2	7.6	7.4	17.4	14.5
Max. Displacement of the Dam Crest (mm)	75	52	30	27	25	42	29	104	78

Table 5 Shear Stresses in right abutment of the arch dam

Elevation	Point	Shear Stresses (MPa)				
		Case I	Case III		Case IV	Case X
		BEM	BEM	FEM	BEM	BEM
0.3 H	A	3.0	1.6	1.5	1.7	2.0
	B	2.9	1.5	1.5	1.5	1.9
	C	2.7	1.3	1.2	1.4	1.8
0.7H	A	2.8	1.3	1.3	2.7	1.9
	B	2.5	1.2	1.1	2.4	1.8
	C	2.1	1.0	1.0	2.2	1.6

analysis of Morrow Point Dam with the foundation rock overlain by a weaker layer indicates that decreasing foundation modulus with elevation generally increases dam deflections and stresses (Table 4). Furthermore, the effects of weaker abutments (zone I) on the dam response are most significant when their moduli are substantially less than the modulus of the concrete.

Bearing in mind that safety of arch dam is much increased once tensile stresses and crest displacement decrease, comparison of cases IX and VIII reveals that, strong abutments are much more influential on arch dam safety, than strong bed rock.

Stability of the abutments is crucial for the safety of arch dam. While unstable wedges of rock in the abutments could endanger the safety of the dam. The abutments are required to resist safely against the thrust imposed upon the dam by the impounded reservoir.

Moreover, the loads that must be considered in the analysis of abutment rock wedges include the weight forces of the rock wedge, (not taken into account in most studies using BEM), thrusts forces of the dam, uplift or buoyancy forces applied to the wedge, and other forces applied due to different loading cases.

Table 5 shows the shear stresses at six points in the abutment of the dam in three cases studied considering foundation self-weight body forces. The points are selected at elevations 0.3H and 0.7H from the base, where H is the dam height. In each elevation three nodes are chosen. Point A is at the intersection of dam intrados with the right abutment; point B and C are at depth "b" and distance "a" of the right abutment respectively as shown in Fig. 8. Previous studies (Federal Energy Regulation Commission, "Chapter 11: Arch Dams" 1999) have shown that the three nodes may contribute to the formation of a sliding wedge in the abutment and need to be checked for the dam stability.

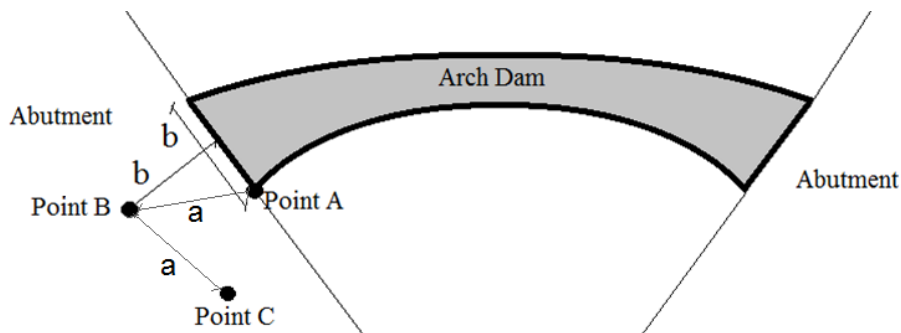


Fig. 8 Schematic plan of arch dam in elevations 0.3H and 0.7H

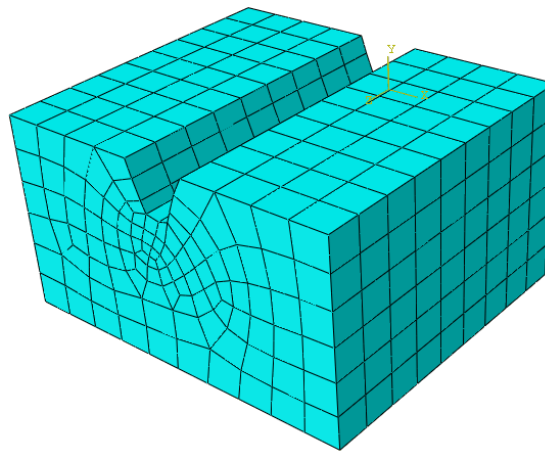


Fig. 9 Finite element model of free field foundation for Morrow Point arch dam

In order to compare the numerical results, especially body forces in infinite domains, free field foundation of Morrow Point arch dam was analyzed by program Abaqus Ver. 6.11. Foundation properties are the same as in case III with the mass density of 2200 kg/m^3 . Its corresponding model consists of 927 20-node brick elements for the foundation. The length of the finite foundation in each direction in finite element model is the same as the boundary element model, and has roller supports in each end to restrain normal displacements as shown in Fig. 9. In this case the system results are achieved by superposing the two analyses results. First, the free-field foundation is analyzed by FEM including body forces load, and subsequently, the complete system is modeled and analysed by the present BEM program with a weightless foundation.

Case X is modeled by a weightless foundation and the same elasticity ratio as in cases III. The latter case is used to clarify the weight effects of the semi-infinite foundation in the dam stability.

Table 5 shows that the results of the boundary element and finite element models have differences up to 9 percent. These differences are attributed to the approximation caused by domain discretization in FEM and the finite boundary conditions.

As the abutments and the foundation properties of Morrow Point arch dam are similar to those of case III and, the corresponding stresses do not seem to exceed the safety criteria (Federal Energy Regulation Commission 1999, 1991) the dam is stable under static loads. However,

stresses of case I may cause dam instability, if a dam of such properties exists. Moreover, as shown in Table 5, eliminating foundation body forces as in case X, leads to unrealistically low stresses estimation and is quite unconservative, thus causing dam instability. Therefore, a careful and precise stability analysis such as the method elaborated in this research may be crucial and must be performed to ensure an adequate factor of safety against abutment sliding.

5. Conclusions

In this research, methods of transforming the volume integral to a surface integral for three-dimensional BEM analysis of unbounded media due to body forces are described along with some applications. The method is verified by comparing against the results of a number of examples with their analytical or numerical solutions. The method is simple to implement and the results are highly accurate in respect to those of finite elements in infinite domains and previous formulations in BEM including body forces. It is demonstrated that elastostatics multi zone problems with infinite or semi-infinite domain including arbitrary body forces could be solved with ease. Moreover, the proposed method is suitable for considering uplift, buoyancy forces, centrifugal forces or any potential functions which could be estimated by a linear function in each domain. Furthermore, some practical applications of the method are presented to show the significance of body forces; sometimes overlooked in BE analysis due to traditional complexity of treatments of such volume integrals. Further development of the proposed method for dynamic loading and indeed in the analysis of nonlinear three-dimensional elastodynamic problems is naturally possible.

References

- Ahmadi, M.T., Izadinia, M. and Bachmann, H. (2001), "A discrete crack joint model for nonlinear dynamic analysis of concrete arch dam", *Int. J. Comput. Struct.*, **79**, 403-420.
- Aliabadi, M.H. (2002), *The Boundary Element Method*, John Wiley & Sons, London, UK.
- Banerjee, P.K. (1994), *The Boundary Element Methods in Engineering*, McGraw-Hill Book Company, London, UK.
- Beer, G. (1993), "An efficient numerical method for modelling initiation and propagation of cracks along material interfaces", *International Journal for Numerical Methods in Engineering*, **36**, 3579-3594.
- Beer, G. and Poulsen, B.A. (1994), "Efficient numerical modeling of faulted rock using the boundary element method", *Int. J. Rock Mech. Min. Sci. Geomech. Abstr.*, **31**(5), 485-506.
- Beer, G., Smith, I. and Duenser, C. (2008), *The Boundary Element Method With Programming*, Springer-Verlag, Wien, Germany.
- Brebbia, A., Talles, J.C.F. and Wrobel, L.C. (1984), *Boundary Element Techniques*, Springer-Verlog, NewYork, USA.
- Cheng, S. and Shuwei, Z. (2012), "Stochastic spline fictitious boundary element method in elastostatic problems with random fields", *Eng. Anal. Bound. Elem.*, **36**(5), 759-771.
- Deb, A. and Banerjee, P.K. (1990), "BEM for general anisotropic 2D elasticity using particular integrals", *Commun. Appl. Numer. Method.*, **6**, 111-119.
- Federal Energy Regulation Commission (1999), *Chapter 11: Arch Dams*, Engineering Guidelines for the Evaluation of Hydropower Projects, Washington D.C, USA.
- Federal Energy Regulation Commission (1991), *Chapter 5: Geotechnical Investigations and Studies*, Engineering Guidelines for the Evaluation of Hydropower Projects, Washington D.C., USA.

- Khodakarami, M.I. and Kaji, N. (2011), "Analysis of elastostatics problems using a semi-analytical method with diagonal coefficient matrices", *Eng. Anal. Bound. Elem.*, **35**, 1288-1296.
- Kuo, H.Y. and Chen, T. (2005), "Steady and transient Green's functions for anisotropic conduction in an exponentially graded solid", *Int. J. Solid. Struct.*, **42**, 1111-1128.
- Leonel, E.D. and Wilson, S.V. (2011), "Non-linear boundary element formulation applied to contact analysis using tangent operator", *Eng. Anal. Bound. Elem.*, **35**, 1237-1247.
- Leonel, E.D. and Wilson, S.V. (2010a), "Dual boundary element formulation applied to analysis of multi-fractured domains", *Eng. Anal. Bound. Elem.*, **34**(12), 1092-1099.
- Leonel, E.D. and Wilson, S.V. (2010b), "Non-linear boundary element formulation with tangent operator to analyse crack propagation", *Eng. Anal. Bound. Elem.*, **34**, 122-129.
- Maerten, F. (2010), "Adaptive cross-approximation applied to the solution of system of equations and post-processing for 3D elastostatic problems using the boundary element method", *Eng. Anal. Bound. Elem.*, **34**(5), 483-491.
- Milroy, J., Hinduja, S. and Davey, K. (1997), "The elastostatics three-dimensional boundary element method: analytical integration for linear isoparametric triangular elements", *Appl. Math. Model.*, **21**, 763-782.
- Ochiai, Y. and Kobayashi, T. (2000), "Stress analysis with arbitrary body force by triple-reciprocity BEM" *Struct. Eng. Mech.*, **10**(4), 393-404.
- Park, K.H. (2002), "A BEM formulation for axisymmetric elasticity with arbitrary body force using particular integrals", *Int. J. Comput. Struct.*, **80**, 2507-2514.
- Park, K.H. and Banerjee, P.K. (2002), "Two- and three-dimensional transient thermoelastic analysis by BEM via particular integrals", *Int. J. Solid. Struct.*, **39**, 2871-2892.
- Pereira, A. and Beer, G. (2009), "Interface dynamic stiffness matrix approach for three-dimensional transient multi-region boundary element analysis", *Int. J. Numer. Method. Eng.*, **80**, 1463-1495.
- Perez-Gavilan, J.J. and Aliabadi, M.H. (2001), "A symmetric galerkin formulation and dual reciprocity for 2D elastostatics", *Eng. Anal. Bound. Elem.*, **25**, 229-235.
- Rodriguez-Tembleque, L. and Abascal, R. (2010) "A 3D FEM-BEM rolling contact formulation for unstructured meshes", *Int. J. Solid. Struct.*, **47**, 330-353.
- Shen, S.Y. (2011), "An indirect elastostatics boundary element method with analytic bases", *Int. J. Comput. Struct.*, **89**, 2402-2413.
- Simpson, R.N., Bordas, S.P.A., Lian, H. and Trevelyan, J. (2013), "An isogeometric boundary element method for elastostatics analysis: 2D implementation aspects", *Int. J. Comput. Struct.*, **118**, 2-12.
- Tang, W.C. and Fenner, R.T. (2005), "Analytical integration and exact geometrical representation in the two-dimensional elastostatics boundary element method", *Appl. Math. Model.* **29**, 1073-1099.
- Timoshenko, S.P. and Goodier, J.N. (1970), *Theory Of Elasticity*, 3rd Edition, McGraw-Hill, New York, USA.